

Antineoplastic Agents 440. Asymmetric Synthesis and Evaluation of the Combretastatin A-1 SAR Probes (1*S*,2*S*)- and (1*R*,2*R*)-1,2-Dihydroxy-1-(2',3'-dihydroxy-4'-methoxyphenyl)-2-(3'',4'',5''-trimethoxyphenyl)-ethane[‡]

George R. Pettit,* John W. Lippert III, Delbert L. Herald, Ernest Hamel,[†] and Robin K. Pettit

Cancer Research Institute and Department of Chemistry Arizona State University, Tempe, Arizona 85287-2404, and Screening Technologies Branch, Developmental Therapeutics Program, Division of Cancer Treatment and Diagnosis, National Cancer Institute, Frederick Cancer Research and Development Center, Frederick, Maryland 21702-1201

Received February 7, 2000

The synthetic (*E*)-isomer (**3b**) of natural combretastatin A-1 (**1a**) isolated from the African bushwillow *Combretum caffrum* was the focus of chiral hydroxylation (Sharpless) reactions as part of a structure–activity relationship study. The resulting (*R,R*)- and (*S,S*)-diols (**6** and **7**) and synthetic intermediates were evaluated against a series of cancer cell lines, microorganisms, and tubulin. Chiral diols **6** and **7** showed increased activity against the P-388 murine lymphocytic leukemia cell line with ED₅₀ values of 3.9 and 2.9 μg/mL, respectively, when compared to the precursor (*E*)-stilbene **3b**. In contrast, (*E*)-stilbene **3b** exhibited more potent antibiotic activity than the chiral diols (**6** and **7**). Both diols, (*R,R*)-**6** and (*S,S*)-**7**, displayed less cancer cell growth inhibition and less antibiotic activity than did natural combretastatin A-1 (**1a**) (P-388 ED₅₀ 0.25 μg/mL).

By 1979, our study of cancer cell growth inhibitory constituents of the African willow tree *Combretum caffrum* Kuntze (Combretaceae)^{1a} was well under way, and, in 1982, we reported the isolation and structure of combretastatin,^{1b,c} the first member of a series of biologically active bibenzyls, stilbenes, and phenanthrenes.^{2a–c} In 1987 and 1989, we reported combretastatins A-1 (**1a**)^{2c} and A-4 (**1b**)^{2d} respectively, which structurally resemble the antimetabolic and cell growth inhibitors colchicine^{3,5} and podophyllotoxin,^{4,5} and represent two of the most promising antineoplastic constituents of *C. caffrum*. Monophenol **1b** proved to be a potent inhibitor of microtubule assembly and exhibited an ED₅₀ value of 7 nM (0.007 μM) against the murine L1210 leukemia cell line,^{2a–d} while diphenol **1a**, which was equally effective as an inhibitor of microtubule assembly (IC₅₀ 2–3 μM), was much less potent as an inhibitor of L1210 cell growth (ED₅₀ 0.6 μM).

Presumably the reduced cytotoxicity to cancer cells shown by diphenol **1a** is due to the presence of its vicinal phenolic groups, which can be easily oxidized to the 1,2-quinone.^{2a,b,5,6} Such an interpretation was supported by the fact that acetylation of the hydroxyl groups enhanced cytotoxicity 10-fold, while significantly reducing the *in vitro* inhibition of tubulin polymerization and colchicine binding.^{2a} Despite these superficial negative aspects, some biological properties exhibited by diphenol **1a** make it attractive. For example, diphenol **1a** may be the most potent antagonist of colchicine binding known, with nearly a 99% inhibition of binding at equal concentrations of inhibitor and [³H] colchicine.^{1d,5} In addition, diphenol **1a** was found to be more potent than monophenol **1b** in its ability to increase intracellular daunorubicin concentrations in multidrug resistant cancer cell lines.⁷ Most importantly, tubulin-binding stilbenes **1a** and **1b** selectively elicit irreversible vascular shutdown within solid tumors.^{8a} The degree of reduction ranged from 50% with **1a** to 70% with **1b**,^{8a} while the combretastatin A-4 prodrug (**1c**), a sodium phosphate

derivative of monophenol **1b**, induced a complete vascular shutdown within metastatic tumors at doses one-tenth of the maximum tolerated dose.^{8b} These very encouraging results indicated that the A-series of combretastatin stilbenes should be further investigated in respect to their antiangiogenic and other anticancer properties. Hence, we initiated a structure–activity relationship (SAR) study of diphenol **1a** to parallel a long-term investigation of the combretastatin A-4 prodrug (**1c**).^{9–11}

Results and Discussion

Previous SAR analyses of the combretastatin A-series indicated that the *cis* configuration of the stilbene unit is the most important factor for inhibition of cancer cell growth.² With the corresponding (*E*)-stilbenes, inhibitory effects on cancer cell growth and tubulin polymerization drop precipitously from effects exhibited by the corresponding (*Z*)-isomers.⁹ Initially, both the *trans* isomers **3b** and **3d** were found to have moderate inhibitory effects on cancer cell growth. Later studies using *trans*-stilbene **3d** revealed that freshly prepared solutions in dimethyl sulfoxide were inactive and gained activity only with the passage of time, suggesting that the *trans* isomer is slowly converted to the active *cis* isomer on storage.¹¹ Bibenzyls **2a** and **2b**, which contain an *sp*³-hybridized freely rotating ethane bridge, exhibit a decrease in antineoplastic activity when compared to the corresponding stilbenes. Recently, we improved the anticancer activity of stilbene **1a** and bibenzyl **2a**, by conversion to the sodium phosphate prodrugs **1d** and **2b**.¹² Both the combretastatin A-1 (**1d**) and B-1 (**2b**) prodrugs exhibit approximately a tenfold increase in cancer cell growth inhibition over their parent compounds, **1a** and **2a** respectively.

The specific purpose of the present investigation was to explore possible conversion of the inactive (*E*)-isomer of combretastatin A-1 into a more active derivative. Recently, we converted the (*E*)-isomer of combretastatin A-4 (**3d**) to chiral diols (*R,R*)-**4** and (*S,S*)-**5**, where the (*E*)-olefin unit was replaced by a freely rotating *sp*³-hybridized chiral ethanediol.^{9a} These experiments have now been extended to include the (*E*)-isomer of combretastatin A-1, generating

* To whom correspondence should be addressed. Tel.: (480) 965-3351. Fax: (480) 965-8558.

[†] Bldg. 469, Room 237, NCI-FCRDC, P.O. Box B, Frederick, MD 21702.

[‡] Dedicated to Professor Norman R. Farnsworth on the occasion of his 70th birthday.

chiral diols (*R,R*)-**6** and (*S,S*)-**7**. Asymmetric dihydroxylation¹³ of *trans*-stilbene **3a**^{2c,12} with AD-mix- α (Sharpless reagent: (DHQ)₂PHAL, K₃Fe(CN)₆, K₂CO₃, K₂O₈·2H₂O) afforded (*S,S*)-diol **8**. Photoisomerization of the (*E*)-stilbene was prevented using an aluminum foil-wrapped reaction vessel.

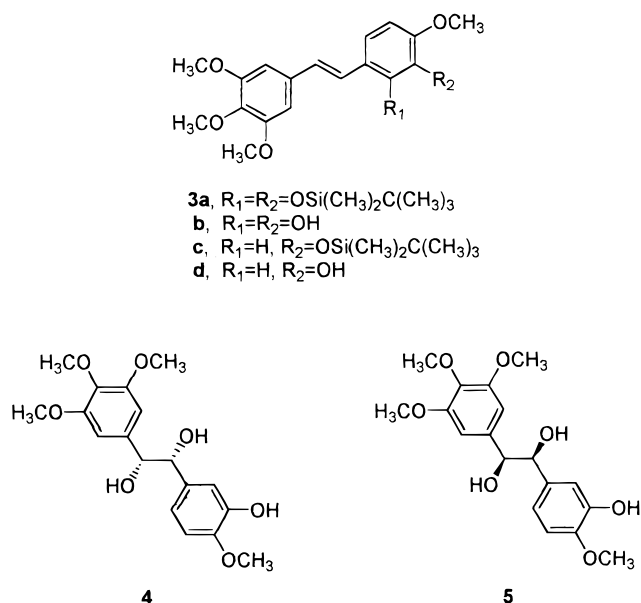
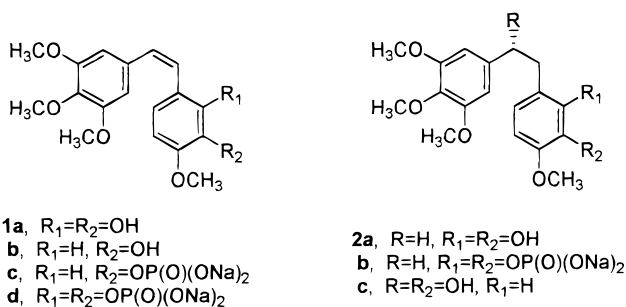


Figure 1. Crystal structure (excluding hydrogens) of (*S,S*)-diol (**8**).

diol **8** with acetic anhydride afforded (*S,S*)-diacetate **10**. Selective desilylation of (*S,S*)-diacetate **10** with TBAF proved to be difficult, yielding several products and suggesting concurrent oxidation.¹⁴ Other methods for desilylation¹⁵ were investigated, but none was able to displace TBAF as the desilylation agent of choice based on its efficient reaction time (ca. 20 min). The (*R,R*)-diols silyl ether **9**, diacetate **11**, and tetraol **6** were prepared analogously using AD-mix- β (DHQD).

A comparison of the diols generated from (*E*)-olefin **3a** revealed a decrease in cancer cell growth inhibition from that of combretastatin A-1 (**1a**), which is consistent with results obtained from the parallel set of diols prepared from the (*E*)-isomer of combretastatin A-4. Interestingly (*S,S*)-diol **5**, a derivative of the *trans* isomer of combretastatin A-4, is significantly more active than (*R,R*)-diol **4** in the cancer cell lines employed (Table 1). In the combretastatin A-1 series, on the other hand, the difference noted in cancer cell line inhibition was negligible, and both (*S,S*)-diol **7** and (*R,R*)-diol **6** were substantially less active than (*S,S*)-diol **5** from the A-4 series.

In previous studies,^{2d} combretastatins A-4 (**1b**) and A-1 (**1a**) had equivalent activities as inhibitors of tubulin polymerization, while combretastatin A-1 appeared to be somewhat more active as an inhibitor of the binding of colchicine to tubulin. Precise analysis of the difference between the two natural products was not possible at that time, and the quantitative results obtained were uncertain because of the marked instability of combretastatin A-1. The synthesis of diols **4**–**7** made possible a reevaluation, albeit indirect, of the relative importance of the second hydroxyl group in the B-ring of the combretastatins. In addition, we have resynthesized combretastatin A-1 and have reevaluated its interactions with tubulin. Table 2 summarizes results obtained with the four diols as inhibitors of tubulin assembly, with a contemporaneous comparison with combretastatins A-4 and A-1. The reaction system currently used¹⁶ yields lower IC₅₀ values than that previously used^{2d} but minimizes the occurrence of aberrant polymerization reactions that often occur with agents that bind to tubulin.¹⁷

The data presented in Table 2 demonstrate that all four diols are much less potent than **1a** and **1b** as inhibitors of tubulin polymerization, in agreement with their much reduced cytotoxicity toward human cancer cell lines. The apparent preference of tubulin for (*S,S*)-diols **5** and **7** versus

As a check that the correct chirality was being induced in the preparation of diols (*R,R*)-**6** and (*S,S*)-**7**, a single-crystal X-ray structure determination was conducted on one of the intermediate silyl-protected products formed in the AD-mix reactions. Thus, treatment of the *trans*-stilbene **3a** with AD-mix- α yielded diol **8**, which was expected to have 1*S*,2*S* absolute stereochemistry. X-ray structure determination of this product (which occurred as the hemihydrate in the solid state) confirmed the expected 1*S*,2*S* stereochemistry. A computer-generated perspective of the silylated diol **8** is shown in Figure 1. Although the absolute stereochemistry of **8** was certain (Flack χ absolute structure parameter = 0.1080 with esd = 0.0492), it was apparent that considerable disorder was present in the solid state of this compound, as evidenced by multiple splitting occurrences for a number of the atoms present in the unit cell. This resulted in the rather poor standard crystallographic residual (*R*₁ of 0.1496) obtained for this structure determination. No attempt was made to further refine the molecules over the multiple occupancy sites, inasmuch as our main objective of confirming the absolute stereochemistry had been met.

Protected diol (*S,S*)-**8** was next desilylated with tetrabutylammonium fluoride (TBAF) to obtain the tetraol (*S,S*)-diol **7** in moderate yield (59%). Reaction of silyl ether (*S,S*)-

Table 1. Human Cancer Cell Line and Murine P-388 Lymphocytic Leukemia Inhibitory Activity of Combretastatins A-1, A-4, B-1, and Synthetic Modifications

compound	leukemia P-388 ED ₅₀ μg/mL	pancreas-ca BXP-3	neuroblast SK-N-SH	thyroid ca SW1736	lung-NSC NCI-H460	pharynx-sq FADU GI ₅₀ μg/mL	prostate DU-145	ovarian OVCAR-3	CNS SF-295	renal A498	colon KM20L2
1a ^a	0.2	4.4	0.19	3.1	0.74	0.23	0.17				
1b	0.0003	0.39	0.0003	0.0007	0.0006	0.0007	0.0008	<0.001	<0.001		0.061
1c	0.0004				0.029			0.023	0.036	0.041	0.34
1d	<0.01	1.5			0.038		0.034	0.024	0.036		0.53
2a	1.7										
2b	0.3	>10			3.3		2.7	2.0	2.3		>10
(<i>R,R</i>)- 4	19.0	>10	1.5	6.1	4.4	2.1	3.5	4.5	5.7	>10	8.2
(<i>S,S</i>)- 5	2.0	3.9	0.28	1.8	2.5	0.60	2.1	0.38	0.52	0.91	0.52
(<i>R,R</i>)- 6	3.9	>10	3.1	>10	7.9	4.9	>10	7.2	2.6	>10	7.0
(<i>S,S</i>)- 7	2.9	>10	3.8	>10	>10	>10	>10	>10	2.9	>10	>10

^a Resynthesis of diphenol **1a** afforded an increase in biological activity from that previously reported in 1987.¹²

Table 2. Inhibition of Tubulin Polymerization by Diols **4–7** and Combretastatin A-4 (**1b**)^a

compound	inhibition of tubulin polymerization IC ₅₀ (μM) ± SD	inhibition of colchicine binding	
		inhibitor:colchicine (% inhibition ± SD)	
		0.2:1	1:1
1a	1.1 ± 0.07	89 ± 3	99.6 ± 0.7
1b	1.0 ± 0.05	81 ± 4	98 ± 1
(<i>R,R</i>)- 4	>40		
(<i>S,S</i>)- 5	14 ± 2		
(<i>R,R</i>)- 6	20 ± 2		
(<i>S,S</i>)- 7	10 ± 2		

^a In the polymerization experiments, the tubulin concentration was 10 μM. In the colchicine binding experiments, the tubulin concentration was 1.0 μM, and the [³H]-colchicine concentration was 5.0 μM. See Verdier-Pinard et al.¹⁶ for further details. All data with **1a** were obtained with solutions prepared immediately before the experiments were performed.

the analogous (*R,R*)-diols **4** and **6** is clear. The (*S,S*)-enantiomer is at least twice as inhibitory as the (*R,R*)-enantiomer. Specifically addressing the question of the importance of the second hydroxyl group in the combretastatin B ring, the results with both the (*R,R*) pair and the (*S,S*) pair support the concept that the strength of the combretastatin interaction with tubulin is enhanced by the presence of the additional hydroxyl moiety. Curiously, the addition of this hydroxyl enhances the interaction with tubulin of the (*R,R*)-diol somewhat more (**6** at least twice as active as **4**) than of the (*S,S*)-diol (**7** only 40% more active than **5**). The greater difference between **4** and **5** than between **6** and **7** in their interactions with tubulin may also account for the greater difference between the former pair and the latter in the cytotoxicity results. However, relative affinities of the four diols for tubulin do not account for the observation that **5** is the most cytotoxic of the four compounds.

In addition, the data in Table 2 confirm the previously observed relative activities of **1a** and **1b**. The differences between the compounds are not great, but **1a** appears to be slightly more active as an inhibitor of colchicine binding.

Against microbe panels, the (*E*)-isomer of combretastatin A-1 (**3b**) was the most active compound, presumably due to its photoisomerization to the active *cis* isomer (Table 3). The difference in antimicrobial activity between parent compounds **1a** and **1b** and their diol derivatives was unremarkable (Table 2).

The premise that the (*Z*)-olefin geometry of the combretastatin stilbenes plays an integral role in the overall biological activity was further supported by the results of this study. In view of the significant astrocyte reversal (9 ASK system) exhibited by the first member of this series, (–)-combretastatin (**2c**),^{1a} the chiral diols herein sum-

Table 3. Antimicrobial Activity of Combretastatins A-1, A-4, B-1, and Synthetic Modifications

compound	microbe(s) inhibited ^a	minimum inhibitory concentration (μg/disk)
1a ^{9a}	<i>S. aureus</i>	50–100
	<i>N. gonorrhoeae</i>	25–50
1b ^{9a}	<i>N. gonorrhoeae</i>	25–50
1c ^{9a}	<i>N. gonorrhoeae</i>	50–100
2a ^{9a}	<i>N. gonorrhoeae</i>	12.5–25
3b	<i>S. aureus</i>	50–100
	<i>S. pneumoniae</i>	50–100
	<i>N. gonorrhoeae</i>	6.25–12.5
	<i>S. maltophilia</i>	50–100
	<i>C. albicans</i>	50–100
	<i>C. neoformans</i>	50–100
3d ^{9a}	^b	
(<i>R,R</i>)- 4 ^{9a}	<i>S. pneumoniae</i>	50–100
(<i>S,S</i>)- 5 ^{9a}	<i>S. pneumoniae</i>	25–50
(<i>R,R</i>)- 6	^b	
(<i>S,S</i>)- 7	<i>N. gonorrhoeae</i>	25–50

^a Each compound was screened against eight bacteria and two fungi as described in the Experimental Section. Only microbes inhibited by <100 μg/disk are listed. ^b At 100 μg/disk, there was no inhibition of the 10 bacteria and fungi tested.

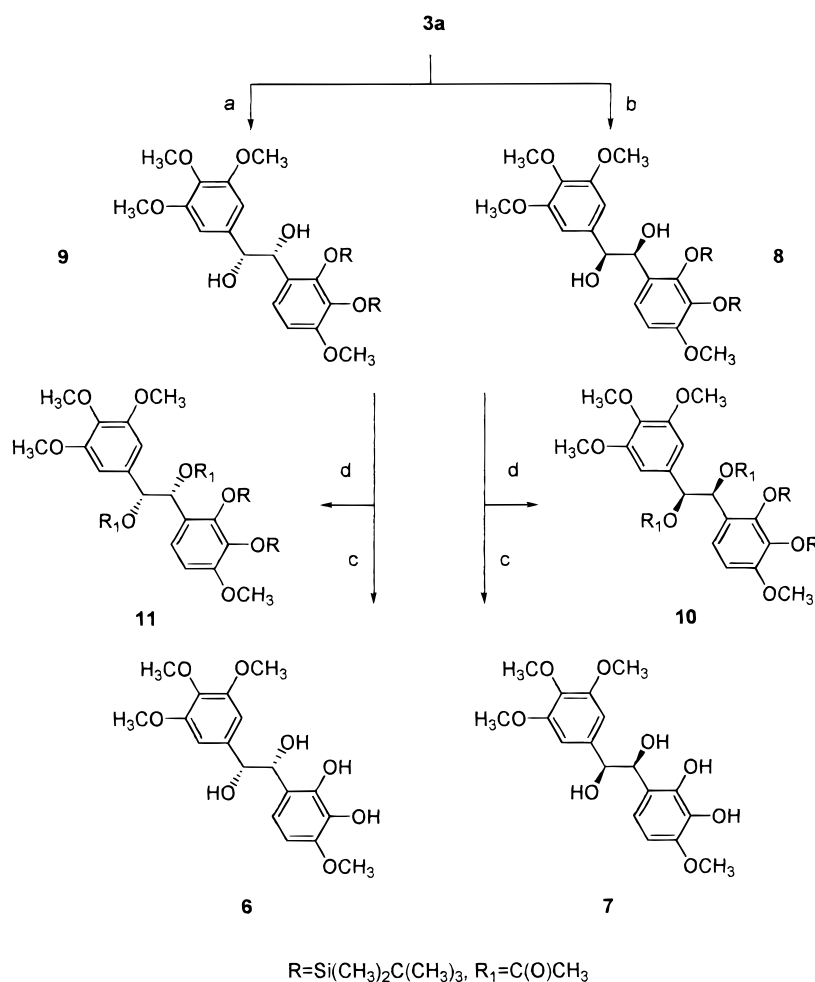
marized may have important biological properties that will eventually be ascertained.

Experimental Section

General Experimental Procedures. Pyridine, acetic anhydride, ethyl acetate (EtOAc), hexane, and CH₂Cl₂ (DCM) were redistilled. TBAF, 4-(dimethylamino)pyridine (DMAP), diisopropylethylamine, and *tert*-butyl alcohol were purchased from the Fisher-Acros Chemical Co., and all other reagents were purchased from the Sigma-Aldrich Chemical Co. Solvent extracts of aqueous solutions were dried over anhydrous sodium sulfate. Column chromatography was performed using either flash Si gel (230–400 mesh ASTM) or gravity Si gel (70–230 mesh ASTM). Analtech Si gel GHLF plates were used for TLC, and all compounds were visualized with fluorescent short-wave light (254 nm).

Melting points were recorded employing an Electrothermal 9100 apparatus and are uncorrected. The ¹H NMR spectra were determined by means of a Varian VXR-300 instrument and are referenced to TMS as the internal standard. Mass spectral data were recorded using a Varian MAT 312 instrument (EIMS), or Vestec Lasertec Research mass spectrometer incorporating a Laser Sciences nitrogen laser (337 nm light pulses of 3-ns duration, with 4-hydroxybenzylidenemalononitrile as the matrix and cytochrome *c* as the external standard for calibration purposes TOFMS).¹⁸ The IR spectra were obtained with a Matteson Instruments 2020 Galaxy Series FTIR instrument. Optical rotation values were recorded employing a Perkin-Elmer 241 polarimeter. The X-ray crystal structure data collection was performed using an Enraf-Nonius

Scheme 1



Reagents and conditions: (a) AD-mix- β , $\text{CH}_3\text{SO}_2\text{NH}_2$, $t\text{-BuOH-H}_2\text{O}$, 0°C ; (b) AD-mix- α , $\text{CH}_3\text{SO}_2\text{NH}_2$, $t\text{-BuOH-H}_2\text{O}$, 0°C ; (c) TBAF, THF; (d) Ac_2O , pyridine, DMAP, DMF.

CAD4 diffractometer. Elemental analyses were determined by Galbraith Laboratories, Inc., Knoxville, TN.

(1*R*,2*R*)-1,2-Dihydroxy-1-[2',3'-di(*tert*-butyldimethylsilyloxy)-4'-methoxyphenyl]-2-(3'',4'',5''-trimethoxyphenyl)ethane (9). To a 100-mL foil-wrapped round-bottom flask containing a magnetic stirbar was added distilled water (14 mL), *tert*-butyl alcohol (14 mL), AD-mix- β (3.8 g; 1.40 g per mmol), and methanesulfonamide (0.27 g; 2.85 mmol). Before being cooled to 0°C , the mixture was stirred at room temperature for several min. Some of the compounds began to precipitate, and 2',3'-bis(*tert*-butyldimethylsilyloxy)-3,4,4',5-tetramethoxy-(*E*)-stilbene (**3a**)¹² (1.4 g; 2.54 mmol) was added at once; the slurry was then stirred vigorously at 0°C for 8 h and at room temperature for 24 h. Sodium sulfite (3.9 g; 30.9 mmol; 12 eq) was added and the mixture stirred for an additional 0.5 h. The product was extracted with EtOAc (4 \times 50 mL), and the combined organic phase was washed with 2 N KOH (aqueous) and dried. Evaporation of the solvent in vacuo produced an off-yellow solid that was absorbed onto Si gel and subjected to flash column chromatography (eluent gradient: 9:1 to 1:1 hexane-EtOAc) to afford a clear oil, which crystallized from hexane as a colorless fluffly solid (0.94 g; 74% based on 0.23 g of **3a** recovered): mp $122\text{--}123^\circ\text{C}$; R_f 0.50 (1:1, hexane-EtOAc); $[\alpha]_D^{25} +46^\circ$ (c 1.2, CHCl_3); IR (Nujol) ν_{max} 3526, 1595, 1251, 1124, 1097, 831, 781 cm^{-1} ; $^1\text{H NMR}$ (300 MHz, CDCl_3) δ -0.16 (3H, s, SiCH_3), -0.050 (3H, s, SiCH_3), 0.040 (3H, s, SiCH_3), 0.17 (3H, s, SiCH_3), 0.89 (9H, s, C_4H_9), 1.01 (9H, s, C_4H_9), 2.45 (1H, d, $J = 1.7$ Hz, OH, D_2O exchanged), 2.89 (1H, d, $J = 1.2$ Hz, OH, D_2O exchanged), 3.72 (6H, s, 2 \times OCH_3), 3.75 (3H, s, OCH_3), 3.76 (3H, s, OCH_3), 4.66 (1H, dd, $J = 7.5$ Hz, $J = 2.4$ Hz, CH), 5.06 (1H, dd, $J = 7.8$ Hz, $J = 3.3$ Hz, CH), 6.33 (2H, s, H-2'', H-6''), 6.59 (1H, d,

$J = 8.1$ Hz, H-5'), 7.05 (1H, d, $J = 8.7$ Hz, H-6'); EIMS m/z 594 (M^+ , 5), 519 (95), 397 (100), 339 (10), 198 (95); *anal.* C 59.70%, H 8.50%, calcd for $\text{C}_{30}\text{H}_{50}\text{O}_8\text{Si}_2 \cdot \frac{1}{2}\text{H}_2\text{O}$, C 59.80%, H 8.50%.

(1*R*,2*R*)-1,2-Dihydroxy-1-(2',3'-dihydroxy-4'-methoxyphenyl)-2-(3'',4'',5''-trimethoxyphenyl)ethane (6). To a solution of (*R,R*)-diol **9** (0.24 g; 0.397 mmol) in anhydrous THF (4 mL), was added TBAF (0.84 μL ; 0.84 mmol; 2.1 eq; 1 M in THF solution) in a previously flame-dried flask. After 20 min the reaction was terminated with ice-cold 6 N HCl and extracted with EtOAc (4 \times 20 mL). The combined organic phase was washed with saturated NaCl (aqueous) and dried. Removal of the organic solvent yielded a dark oil, which was subjected to column chromatography (66:33:1 EtOAc-hexane-HOAc) to afford a light brown oil that crystallized from EtOAc-hexane as a colorless solid (75 mg; 52%): mp $64\text{--}66^\circ\text{C}$; R_f 0.36 (66:33:1, hexane-EtOAc-HOAc); $[\alpha]_D^{25} +56^\circ$ (c 1.1, CHCl_3); IR (film) ν_{max} 3425, 2939, 1593, 1454, 1327, 1234, 1145 cm^{-1} ; $^1\text{H NMR}$ (300 MHz, CDCl_3) δ 3.70 (6H, s, 2 \times OCH_3), 3.79 (3H, s, OCH_3), 3.80 (3H, s, OCH_3), 4.67 (1H, d, $J = 7.8$ Hz, CH), 4.83 (1H, d, $J = 7.2$ Hz, CH), 6.12 (1H, d, $J = 8.7$ Hz, H-5'), 6.24 (1H, d, $J = 9.0$ Hz, H-6'), 6.33 (2H, s, H-2'', H-6''); EIMS m/z 348 ($\text{M}^+ - \text{H}_2\text{O}$, 60), 319 (95), 196 (100), 167 (10), 153 (25); *anal.* C 57.59%, H 6.18%, calcd for $\text{C}_{18}\text{H}_{22}\text{O}_8 \cdot \frac{1}{2}\text{H}_2\text{O}$, C 57.41%, H 6.25%.

(1*S*,2*S*)-1,2-Dihydroxy-1-[2',3'-di(*tert*-butyldimethylsilyloxy)-4'-methoxyphenyl]-2-(3'',4'',5''-trimethoxyphenyl)ethane (8). The asymmetric dihydroxylation reaction conditions described above for preparation of (*R,R*)-diol **9** were applied to (*E*)-olefin **3a** (1.56 g; 2.78 mmol) using AD-mix- α to afford (*S,S*)-diol **8** as a colorless fluffly solid (1.2 g; 75%): mp $122\text{--}123^\circ\text{C}$; R_f 0.50 (1:1, hexane-EtOAc); $[\alpha]_D^{25} -46^\circ$ (c 1.3,

CHCl₃); IR (Nujol) ν_{\max} 3524, 2361, 1593, 1251, 1124, 1097, 954, 831 cm⁻¹; ¹H NMR (300 MHz, CDCl₃) δ -0.16 (3H, s, SiCH₃), -0.05 (3H, s, SiCH₃), 0.04 (3H, s, SiCH₃), 0.17 (3H, s, SiCH₃), 0.89 (9H, s, C₄H₉), 1.01 (9H, s, C₄H₉), 2.44 (1H, d, J = 3.3 Hz, OH, D₂O exchanged), 2.87 (1H, d, J = 1.2 Hz, OH, D₂O exchanged), 3.72 (6H, s, 2 × OCH₃), 3.75 (3H, s, OCH₃), 3.76 (3H, s, OCH₃), 4.66 (1H, dd, J = 7.8 Hz, J = 2.1 Hz, CH), 5.06 (1H, dd, J = 7.5 Hz, J = 3.3 Hz, CH), 6.33 (2H, s, H-2'', H-6''), 6.59 (1H, d, J = 8.7 Hz, H-5'), 7.06 (1H, d, J = 8.4 Hz, H-6'); EIMS m/z 594 (M⁺, 10), 519 (95), 397 (100), 339 (20), 198 (100); *anal.* C 59.70%, H 8.50%, calcd for C₃₀H₅₀O₈Si₂· $\frac{1}{2}$ H₂O, C 59.66%, H 8.61%.

X-ray Crystal Structure of (1*S*,2*S*)-1,2-Dihydroxy-1-[2',3'-bis(*tert*-butyldimethylsilyloxy)-4'-methoxyphenyl]-2-(3'',4'',5''-trimethoxyphenyl)-ethane hemihydrate (8). A thin plate, 0.40 × 0.40 × 0.06 mm, obtained from a MeOH-hexane solution, was mounted on the tip of a glass fiber with Super Glue. Data collection was performed at 27 ± 1° for a monoclinic system, with all reflections corresponding to slightly more than a complete quadrant ($2\theta \leq 130^\circ$) being measured using an $\omega/2\theta$ scan technique. Friedel reflections were also collected, whenever possible, immediately after each original reflection. Subsequent statistical analysis of the complete reflection data set using the XPREP¹⁹ program indicated the space group was *P*2₁. Each asymmetric unit of the cell was found to contain four independent molecules of the parent molecule, as well as two molecules of water. Crystal data: C₃₀H₅₀O₈· $\frac{1}{2}$ H₂O, a = 13.303(2), b = 32.475(7), c = 19.960(4) Å, V = 7179(3) Å³, λ (Cu K α) = 1.54178 Å, ρ_c = 1.117 g cm⁻³ for Z = 8 and fw = 603.89, $F(000)$ = 2616. After Lorentz and polarization corrections, merging of equivalent reflections and rejection of systematic absences, 19 017 unique reflections [$R(\text{int}) = 0.1195$] remained, of which 13 433 were considered observed [$I_o > 2\sigma(I_o)$] and were used in the subsequent structure solution and refinement. Linear and anisotropic decay corrections were applied to the intensity data as well as an empirical absorption correction (based on a series of ψ -scans).²⁰ Structure determination was accomplished with SHELXS.¹⁹ All non-hydrogen atoms for **8**, including the water-solvate atoms, were located using the default settings of that program. The remaining hydrogen atom positions were calculated at optimal positions. The latter atoms were assigned thermal parameters equal to 1.2 or 1.5 (depending upon structural atom type) of the U_{iso} value of the atom to which they were attached, and then both coordinates and thermal values were forced to ride that atom during final cycles of refinement. All non-hydrogen atoms were refined anisotropically in a full-matrix least-squares refinement process with SHELXL¹⁹ in the SHELXTL-PC software package. The final standard residual R value for the model shown in Figure 1 was 0.1484 for observed data (13 433 reflections) and 0.1850 for all data (19 017 reflections). The corresponding Sheldrick R values were wR_2 of 0.3706 and 0.4031, respectively. The Flack absolute structure parameter χ was 0.05 (5) for the model depicted in Figure 1, thus indicating that the absolute stereochemistry shown (and expected) for **8** is correct (i.e., 1*S*, 2*S*). A final difference Fourier map showed residual electron density attributed solely to the silicon atoms; the largest difference peak and hole being 0.61 and -0.55 e/Å³, respectively. Final bond distances and angles were all within acceptable limits.²¹

(1*S*,2*S*)-1,2-Dihydroxy-1-(2',3'-dihydroxy-4'-methoxyphenyl)-2-(3'',4'',5''-trimethoxyphenyl)-ethane (7). Silyl ether (*S,S*)-diol **8** (0.36 g; 0.610 mmol) was desilylated as described above for the synthesis of (*R,R*)-diol **6** and afforded (*S,S*)-diol **7** as a colorless solid (0.13 g; 59%): mp 64–66 °C; R_f 0.36 (66:33:1 hexane-EtOAc-HOAc); $[\alpha]_D^{25}$ -52° (c 0.99, CHCl₃); IR (film) ν_{\max} 3418, 2939, 1593, 1510, 1462, 1327, 1290, 1234, 1124 cm⁻¹; ¹H NMR (300 MHz, CDCl₃) δ 3.73 (6H, s, 2 × OCH₃), 3.81 (3H, s, OCH₃), 3.83 (3H, s, OCH₃), 4.70 (1H, d, J = 7.2 Hz, CH), 4.88 (1H, d, J = 7.2 Hz, CH), 6.15 (1H, d, J = 8.1 Hz, H-5'), 6.27 (1H, d, J = 8.1 Hz, H-6'), 6.37 (2H, s, H-2'', H-6''); EIMS m/z 348 (M⁺ - H₂O, 20), 319 (15), 196 (100), 168 (20), 153 (10); *anal.* C 57.59%, H 6.18%, calcd for C₁₈H₂₂O₈· $\frac{1}{2}$ H₂O, C 57.61%, H 6.28%.

(1*R*,2*R*)-1,2-Diacetoxy-1-[2',3'-di(*tert*-butyldimethylsilyloxy)-4'-methoxyphenyl]-2-(3'',4'',5''-trimethoxyphenyl)-ethane (11). To a solution of (*R,R*)-diol **9** (0.21 g; 0.351 mmol) in anhydrous DCM (2 mL) was added acetic anhydride (26 mL; 2.7 mmol; 7.8 eq), pyridine (0.20 mL; 2.35 mmol; 6.7 eq), and a catalytic amount of DMAP (5 mg). After 3 h, the reaction was terminated with ice-water and extracted with EtOAc (4 × 25 mL). The combined organic phase was washed with 2 N HCl followed by 10% NaHCO₃ (aqueous) and dried. Removal (reduced pressure) of solvent yielded a clear oil that was separated by flash column chromatography (1:1 hexane-EtOAc) to afford a crude product, which crystallized from hexane as a colorless solid (0.24 g; 99%): mp 128–129 °C; R_f 0.63 (2:1, hexane-EtOAc); $[\alpha]_D^{25}$ -22° (c 1.4, CHCl₃); EIMS m/z 678 (M⁺, 5), 621 (40), 439 (60), 397 (100), 73 (30); *anal.* C 60.14%, H 8.01%, calcd for C₃₄H₅₄O₁₀Si₂, C 60.38%, H 8.09%.

(1*S*,2*S*)-1,2-Diacetoxy-[2',3'-di(*tert*-butyldimethylsilyloxy)-4'-methoxyphenyl]-2-(3'',4'',5''-trimethoxyphenyl)-ethane (10). The silyl ether (*S,S*)-diol **8** (0.25 g; 0.42 mmol) was acylated as described above for the synthesis of (*R,R*)-diacetate **11** to afford a colorless solid (0.28 g; 98%): mp 128–129 °C; R_f 0.63 (2:1, hexane-EtOAc); $[\alpha]_D^{25}$ +20° (c 1.3, CHCl₃); TOFMS m/z 717, (M + K)⁺; *anal.* C 60.14%, H 8.01%, calcd for C₃₄H₅₄O₁₀Si₂, C 60.08%, H 8.08%.

Tubulin Assays. The tubulin polymerization and colchicine binding experiments were performed as described previously.¹⁶ However, in the polymerization assays Beckman DU7400/7500 spectrophotometers equipped with "high-performance" temperature controllers were used. These instruments are micro-processor controlled, and assays required use of programs provided by MDB Analytical Associates, South Plainfield, NJ.

Antimicrobial Susceptibility Testing. Compounds were screened against the bacteria *Stenotrophomonas maltophilia*, *Micrococcus luteus*, *Staphylococcus aureus*, *Escherichia coli*, *Enterobacter cloacae*, *Enterococcus faecalis*, *Streptococcus pneumoniae*, and *Neisseria gonorrhoeae*, and the fungi *Candida albicans* and *Cryptococcus neoformans*, according to established disk susceptibility testing protocols.²²

Acknowledgment. Thanks and appreciation for support of this research are directed to Outstanding Investigator Grant CA 44344-6-11 with the Division of Cancer Treatment and Diagnosis, NCI, DHHS; the Arizona Disease Control Research Commission; Diane Cummings Halle; Gary L. and Diane R. Tooker; Polly Trautman; the Caitlin Robb Foundation, and the Robert B. Dalton Endowment. We are pleased to thank for other assistance Drs. Cherry L. Herald, Fiona Hogan, Jean M. Schmidt, and J. Charles Chapuis, as well as Laura Crews and Lee Williams.

Supporting Information Available: X-ray data for **8**. This material is available free of charge via the Internet at <http://acs.pubs.org>.

References and Notes

- (a) Pettit, G. R.; Singh, S. B.; Cragg, G. M. *J. Org. Chem.* **1985**, *50*, 3404–3406 and Pettit, G. R.; Cragg, G. M.; Herald, D. L.; Schmidt, J. M.; Lohavanijaya, P. *Can. J. Chem.* **1982**, *60*, 1374–1376. (b) Hutchings, A.; Scott, A. H.; Lewis, G.; Cunningham, A. B. *Zulu Medicinal Plants, an Inventory*; University of Natal Press: South Africa, 1996; p 214. (c) Pettit, G. R.; Cragg, G. M.; Singh, S. B. *J. Nat. Prod.* **1987**, *50*, 386–391. (d) Pettit, R. K.; Hamel, E.; Hazen, K.; Pettit, G. R.; Crews, L. C. *Antimicrob. Agents Chemother.*, in preparation.
- (a) Pettit, G. R.; Singh, S. B.; Boyd, M. R.; Hamel, E.; Pettit, R. K.; Schmidt, J. M.; Hogan, F. *J. Med. Chem.* **1995**, *38*, 1666–1672. (b) Hamel, E. *Med. Res. Rev.* **1996**, *16*, 207–231. (c) Pettit, G. R.; Singh, S. B.; Niven, M. L.; Hamel, E.; Schmidt, J. M. *J. Nat. Prod.* **1987**, *50*, 119–131. (d) Pettit, G. R.; Singh, S. B.; Hamel, E.; Lin, C. M.; Alberts, D. S.; Garcia-Kendall, D. *Experientia* **1989**, *45*, 209–211, and Lin, C. M.; Singh, S. B.; Ping, S. C.; Dempsey, R. O.; Schmidt, J. M.; Pettit, G. R.; Hamel, E. *Mol. Pharm.* **1988**, *34*, 200–208. (e) Pettit, G. R.; Singh, S. B.; Schmidt, J. M. *Nat. Prod.* **1988**, *51*, 517–527. (f) Nandy, P.; Samitendu, B.; Gao, H.; Hui, M. B. V.; Lien, E. *J. Pharm. Res.* **1991**, *8*, 776–781. (g) Roberson, R. W.; Tucker, B.; Pettit, G. R. *Mycol. Res.* **1998**, *102*, 378–382.
- Boye, O.; Brossi, A. In *The Alkaloids*; Brossi, A., Cordell, G. A., Eds.; Academic: New York, 1992; Vol. 41, pp 125–178.
- Bush, E. J.; Jones, D. W. *J. Chem. Soc., Perkin Trans. 1* **1995**, 151–155.

- (5) Sackett, D. L. *Pharmacol. Ther.* **1993**, *59*, 163–228.
- (6) (a) Pelizzoni, F.; Verotta, L.; Rogers, C. B.; Colombo, R.; Pedrotti, B.; Balconi, G.; Erba, E.; D'Incalci, M. *Nat. Prod. Lett.* **1993**, *1*, 273–280. (b) Orsini, F.; Pelizzoni, F.; Bellini, B.; Miglierini, G. *Carbohydr. Res.* **1997**, *301*, 95–109.
- (7) McGown, A. T.; Fox, B. W. *Cancer Chemother. Pharmacol.* **1990**, *26*, 79–81.
- (8) (a) Chaplin, D. J.; Pettit, G. R.; Parkins, C. S.; Hill, S. A. *Br. J. Cancer* **1996**, *74*, S86–S88. (b) Dark, G. G.; Hill, S. A.; Prise, V. E.; Tozer, G. M.; Pettit, G. R.; Chaplin, D. J. *Cancer Res.* **1997**, *57*, 1829–1834.
- (9) (a) Pettit, G. R.; Toki, B. E.; Herald, D. L.; Boyd, M. R.; Hamel, E.; Pettit, R. K.; Chapuis, J.-C. *J. Med. Chem.* **1999**, *42*, 1459–1465. (b) Pettit, G. R.; Rhodes, M. R.; Herald, D. L.; Chaplin, D. J.; Stratford, M. R. L.; Hamel, E.; Pettit, R. K.; Chapuis, J.-C.; Oliva, D. *Anti-Cancer Drug Des.* **1998**, *13*, 981–993. (c) Pinney, K. G.; Bounds, A. D.; Dingeman, K. M.; Mocharla, V. P.; Pettit, G. R.; Bai, R.; Hamel, E. *Bioorg. Med. Chem. Lett.* **1999**, *9*, 1081–1086.
- (10) (a) Hatanaka, T.; Fujita, K.; Ohsumi, K.; Nakagawa, R.; Fukuda, Y.; Nihei, Y.; Suga, Y.; Akiyama, Y.; Tsuji, T. *Bioorg. Med. Chem. Lett.* **1998**, *8*, 3371–3374. (b) Ohsumi, K.; Hatanaka, T.; Fujita, K.; Nakagawa, R.; Fukuda, Y.; Nihei, Y.; Suga, Y.; Morinaga, Y.; Akiyama, Y.; Tsuji, T. *Bioorg. Med. Chem. Lett.* **1998**, *8*, 3153–3158. (c) Ohsumi, K.; Nakagawa, R.; Yumiko, F.; Hatanaka, T.; Morinaga, Y.; Nihei, Y.; Ohishi, K.; Suga, Y.; Akiyama, Y.; Tsuji, T. *J. Med. Chem.* **1998**, *41*, 3022–3032. (d) Medarde, M.; Ramos, A.; Caballero, E.; Pelaez-Lamamie de Clairac, R.; Lopez, J. L.; Gravalos, D. G.; Feliciano, A. S. *Eur. J. Med. Chem.* **1998**, *33*, 71–77.
- (11) (a) Cushman, M.; Nagarathnam, D.; Gopal, D.; Chakraborti, A. K.; Lin, C. M.; Hamel, E. *J. Med. Chem.* **1991**, *34*, 2579–2588. (b) Cushman, M.; Nagarathnam, D.; Gopal, D.; He, H.-M.; Lin, C. M.; Hamel, E. *J. Med. Chem.* **1992**, *35*, 2293–2306.
- (12) Pettit, G. R.; Lippert, J. W., III. *Anti Cancer Drug Des.* in press.
- (13) (a) Kolb, H. C.; VanNieuwenhze, M. S.; Sharpless, K. B. *Chem. Rev.* **1994**, *94*, 2483–2547. (b) Sharpless, K. B.; Amberg, W.; Bennani, Y. L.; Crispino, G. A.; Hartung, J.; Jeong, K.-S.; Kwong, H.-L.; Morikawa, K.; Wang, Z.-M.; Xu, D.; Zhang, X.-L. *J. Org. Chem.* **1992**, *57*, 2768–2771. (c) Harcken, C.; Bruckner, R.; Rank, E. *Chem.—Eur. J.* **1998**, *4*, 2342–2352. (d) Hajamis, U. D.; Gadre, J. N.; Pednekar, S. *Indian J. Chem., Sect. B* **1998**, *37*, 925–928. (e) Gypser, A.; Michel, D.; Nirschl, D. S.; Sharpless, K. B. *J. Org. Chem.* **1998**, *63*, 7322–7327.
- (f) Xie, L.; Takeuchi, Y.; Cosentino, L. M.; Lee, K. H. *Biorg. Med. Chem. Lett.* **1998**, *8*, 2151–2156. (g) Trost, B. M.; Lee, C. B. *J. Am. Chem. Soc.* **1998**, *120*, 6818–6819. (h) Sinha, S. C.; Sinha, A.; Sinha, S. C.; Keinan, E. *J. Am. Chem. Soc.* **1998**, *120*, 4017–4018. (i) Marshall, J. A.; Hinkle, K. W. *Tetrahedron Lett.* **1998**, *39*, 1303–1306.
- (14) Haines, A. H. In *Methods for Oxidation of Organic Compounds*; Academic: New York, 1988; Vol. 2, pp 305–323, 438–447.
- (15) (a) Sinhababu, A. K.; Kawase, M.; Borchardt, R. T. *Synthesis* **1988**, 710–711. (b) Nelson, T. D.; Crouch, D. *Synthesis* **1996**, 1031–1069.
- (16) Verdier-Pinard, P.; Lai, J.-Y.; Yoo, H.-D.; Yu, J.; Marquez, B.; Nagle, D. G.; Nambu, M.; White, J. D.; Falck, J. R.; Gerwick, W. H.; Day, B. W.; Hamel, E. *Mol. Pharmacol.* **1998**, *53*, 62–76.
- (17) (a) Hamel, E.; Blokhin, A. V.; Nagle, D. G.; Yoo, H.-D.; Gerwick, W. H. *Drug Dev. Res.* **1995**, *34*, 110–120. (b) Bai, R.; Durso, N. A.; Sackett, D. L.; Hamel, E. *Biochemistry* **1999**, *38*, 14302–14310.
- (18) Brune, D. C.; Cheung, J. *Proceedings of the 45th ASMS Conference on Mass Spectrometry and Allied Topics*, Palm Springs, CA, June 1–5, 1997.
- (19) SHELXTL-PC, Version 5.1, 1997, an integrated software system for the determination of crystal structures from diffraction data, Bruker Analytical X-ray Systems, Inc.: Madison, WI, 1997. This package includes, among others: XPREP, an automatic space group determination program; XS, the Bruker SHELXS module for the solution of X-ray crystal structures from diffraction data; XL, the Bruker SHELXL module for structure refinement; XP, the Bruker interactive graphics display module for crystal structures.
- (20) North, A. C.; Phillips, D. C.; Mathews, F. S. *Acta Crystallogr.* **1968**, *A24*, 351–359.
- (21) Crystallographic data for the structure(s) reported in this paper have been deposited with the Cambridge Crystallographic Data Centre. Copies of the data can be obtained, free of charge, on application to the Director, CCDC, 12 Union Road, Cambridge CB2 1EZ, UK (fax: +44-(0)1223-336033 or e-mail: deposit@ccdc.cam.ac.uk).
- (22) National Committee for Clinical Laboratory Standards 1997. Performance standards for antimicrobial disk susceptibility tests-sixth edition: Approved Standard M2-A6, NCCLS, Wayne, PA.

NP0000623